

Electron transport signature of H₂ dissociation on atomic gold wires

Alexandre Zanchet,[†] Anaís Dorta-Urra,[†] Octavio Roncero,[†] Alfredo Aguado,[‡]
José Ignacio Martínez,[¶] Fernando Flores,[§] and Nicolás Lorente ^{*,||}

Unidad Asociada UAM-CSIC, Instituto de Física Fundamental, CSIC Serrano 123, 28006 Madrid, Spain., Unidad Asociada UAM-CSIC, Departamento de Química Física, Facultad de Ciencias C–XIV, Universidad Autónoma de Madrid, 28049 Madrid, Spain., Dept. de Superficies y Recubrimientos, Instituto de Ciencia de Materiales de Madrid (CSIC), ES-28049, Madrid, Spain, Departamento de Física Teórica de la Materia Condensada, Facultad de Ciencias C-V, Universidad Autónoma de Madrid, 28049, Madrid, Spain , ICN2 - Institut Catala de Nanociencia i Nanotecnologia, Campus UAB, 08193 Bellaterra (Barcelona), Spain , and CSIC - Consejo Superior de Investigaciones Científicas, ICN2 Building, 08193 Bellaterra (Barcelona), Spain

E-mail: nicolas.lorente@cin2.cat

*To whom correspondence should be addressed

[†]Unidad Asociada UAM-CSIC, Instituto de Física Fundamental, CSIC Serrano 123, 28006 Madrid, Spain.

[‡]Unidad Asociada UAM-CSIC, Departamento de Química Física, Facultad de Ciencias C–XIV, Universidad Autónoma de Madrid, 28049 Madrid, Spain.

[¶]Dept. de Superficies y Recubrimientos, Instituto de Ciencia de Materiales de Madrid (CSIC), ES-28049, Madrid, Spain

[§]Departamento de Física Teórica de la Materia Condensada, Facultad de Ciencias C-V, Universidad Autónoma de Madrid, 28049, Madrid, Spain

^{||}ICN2 - Institut Catala de Nanociencia i Nanotecnologia, Campus UAB, 08193 Bellaterra (Barcelona), Spain

[⊥]CSIC - Consejo Superior de Investigaciones Científicas, ICN2 Building, 08193 Bellaterra (Barcelona), Spain

Abstract

Non-equilibrium Green's functions calculations based on density functional theory show a direct link between the initial stages of H₂ dissociation on a gold atomic wire and the electronic current supported by the gold wire. The simulations reveal that for biases below the stability threshold of the wire, the minimum-energy path for H₂ dissociation is not affected. However, the electronic current presents a dramatic drop when the molecule initiates its dissociation. This current drop is traced back to quantum interference between electron paths when the molecule starts interacting with the gold wire.

The field of molecular dynamics studied by electronic currents has been continuously expanding in the last two decades.¹⁻⁸ Major progress was achieved, when electron currents were tailored to detect reactions within a single molecule, prompting the search for single-molecule chemistry.⁹⁻¹¹ In this way, molecules could be studied to dissociate,² to assemble,^{4,5} to desorb^{10,11} in the extraordinary conditions of a perfectly known environment. All of these experiments were performed for molecular adsorbates under a scanning tunneling microscope tip. However, no electrical probe has been proposed to study single-molecule chemistry in gas phase or in solution.

Using the variations of electronic currents in nanowires is a very interesting possibility for reaching the single-molecule limit in gas or liquid chemical reactions. Due to the extreme reduction in the wire's dimensions, nanowires present enhanced reactivity. Thus, the very inert noble metal, gold, becomes chemically active in clusters¹²⁻²¹ and nanowires²²⁻²⁹ due to the presence of many dangling orbitals which form bonds with surrounding molecules. In particular, the possible dissociation of H₂ on gold nanowires has already been reported.^{30,31} In order to use the nanowire as a reactivity sensor, the electronic transport properties of the wire should change in presence of a chemical reaction while the reaction remains unaltered by the flowing electron current. Unfortunately, no evidence of the reactivity-sensing properties of atom-size nanowires has been revealed yet.

In this Letter, we concurrently evaluate the minimum-energy path (MEP) of a gas-phase H₂ molecule that impinges on a gold nanowire and the wire's electron current, using non-equilibrium

Green's functions (NEGF) and density functional theory (DFT). These calculations show that for biases below the stability threshold of the wire, the H₂ molecular dynamics is not affected. However, the electronic current presents a dramatic drop when the molecule initiates its dissociation. Hence, atom-size nanowires can be excellent probes for determining the onset of H₂ dissociation without perturbation from the measuring current.

Starting from an initial atomic configuration, the MEP is obtained by computing the total potential energy and its gradient as the H₂ molecule approaches the atomic wire. The initial configuration corresponds to H₂ far from a gold monoatomic wire and the final one corresponds to the chemisorbed species on the wire, forming the usual Au-H-Au-H-Au double-bridge bond.³¹ The energy and corresponding gradients are evaluated using the TRANSIESTA code^{32,33} with the Perdew, Burke and Ernzerhof (PBE96) functional.³⁴ The whole system can be divided in three distinct regions breaking periodicity along the transport direction. The contact region is a central region composed of a 4-atom free-standing gold chain connected to two electrodes, left and right, each formed by the first 5 layers of a 3 × 3 cell of Au (111). The two electrodes were frozen, and kept at a distance of 13.3 Å. The inter-electrode distance affects the inter-atomic distance, which has been analyzed elsewhere.²⁸ The other two regions are the semi-infinite electrodes formed by periodically repeating 3 layers of bulk gold in the (111) direction. In this way, bias can be applied between the two asymptotic regions by shifting their Fermi levels, and by self-consistently solving the Poisson and DFT equations for the non-equilibrium density matrix in the central region.³³ Finally, the electron transmission through the central region is evaluated for all cases using standard non-equilibrium Green's functions.³³

Three different models of the wire, of decreasing complexity, have been built to better understand the processes under study, and in each case a MEP has been calculated. First, the model contact described above in which the 4 central gold and the two hydrogen atoms are optimized along the MEP (relaxed wire). In the second case, the 4 central gold atoms are kept frozen in a linear configuration, and only the geometry of the two hydrogen atoms are optimized (frozen wire). Finally, we consider the case of a linear chain of 12 gold atoms (linear wire), repeated periodi-

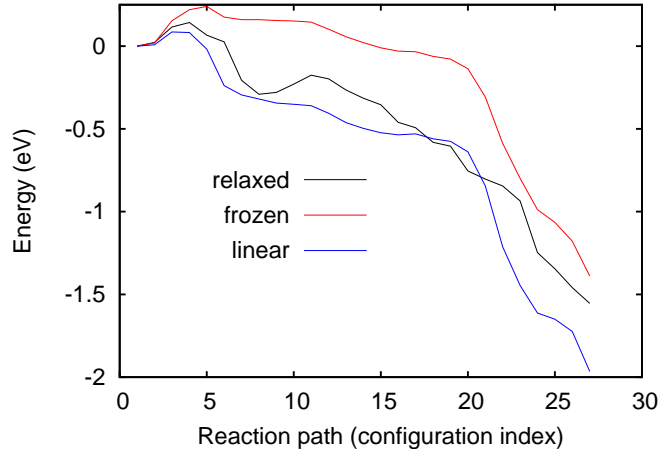


Figure 1: (Color online) Minimum-energy path (MEP) for three models of a hydrogen molecule impinging on a 4-atom gold wire connected to semi-infinite electrodes. The energy with respect to the initial configuration energy is plotted against the index of the sequence of minimum-energy configurations of the H_2 -wire system. The initial configuration corresponds to relaxed molecule and wire distant enough to have no mutual interaction. Black line (relaxed): MEP when the 4-atom chain is also allowed to change its geometry. Red line (frozen): MEP for a frozen 4-atom chain to the initial configuration. Blue line (linear): MEP for an infinite gold atom chain that is allowed to adapt to the evolving H_2 molecule. The realistic case (relaxed) shows two equilibrium situations at the stages $i=8$ and $i=27$ of the MEP.

cally, kept frozen and where only the two hydrogen atoms define the MEP. The MEP in the three considered cases have been discretized in a set of 27 points, each one corresponding to a different nuclear configuration. The initial stage, $i=1$, corresponds to the H_2 far from the wire, while $i = 27$ corresponds to the hydrogen atoms chemisorbed on the wire in the Au-H-Au-H-Au double-bridge bond. In between these two limiting configurations, the label i denotes similar geometries for the three MEPs considered as shown in 1

In the three cases, H_2 dissociation on the gold wire is exothermic by 1.4-2 eV. All the cases present a low barrier when H_2 approaches the wire (approximately at $i=4$). The barrier height is ≈ 0.12 eV for the relaxed and linear wires and ≈ 0.25 eV for the frozen case. Keeping in mind that the zero-point energy of H_2 is ≈ 0.25 eV, it should be easy to overpass. Once on the top of this barrier, the reaction path has been determined by following the gradient. In the case of the

relaxed wire, there is a well for $i=8$, of roughly 0.25 eV below the asymptote given by $i=1$. Some characteristic geometries for the relaxed and frozen wires are illustrated in the lateral panels of 2

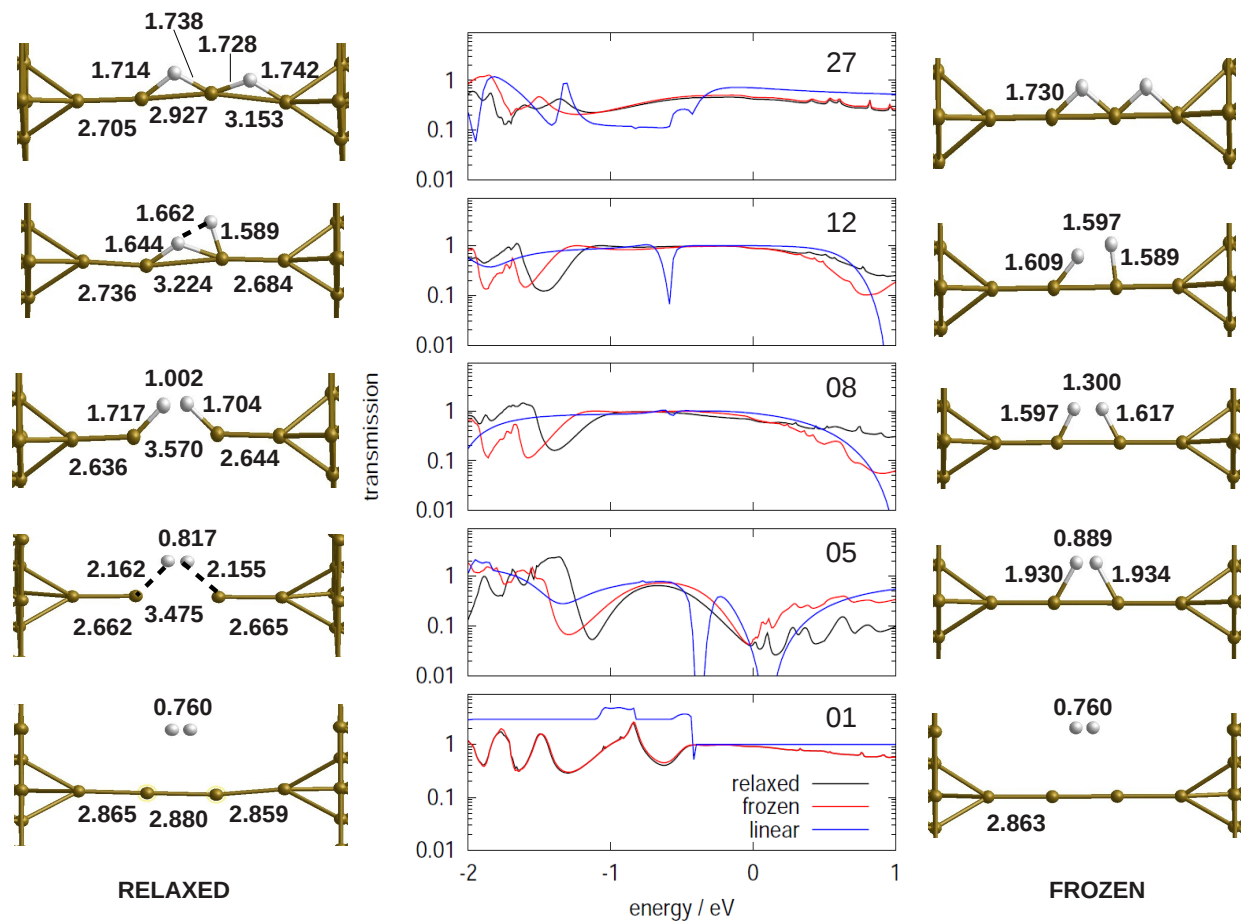


Figure 2: (Color online) Central panels: electronic transmission versus electronic energy at significant points along the H_2 MEP. The zero of energy is taken at the electrode's Fermi level. In the lateral panels, the geometries of the relaxed (left) and frozen (right) wires are shown. The geometries of the infinite linear gold wire are very similar to those of the frozen wire. Numbers in the geometrical schemes denote distances in Å. The spontaneous H_2 dissociation is initiated at stage $i=5$, where the transmission shows an important decrease at the Fermi level.

We can now evaluate the electron transmission between electrodes for each of the stages, i , of the MEP. When H_2 is far from the wire, $i = 1$ bottom panel of 2, the transmission at the Fermi level is equal to one for the three cases because each system presents one single conduction channel. On the opposite side, for $i=27$ with the two hydrogen atoms chemisorbed in the wire forming the double-bridge bond, the transmission is reduced, being ≈ 0.75 in the linear model and ≈ 0.5 in the other two cases. At the minimum ($i=8$) and saddle ($i=12$) points the transmission is in between

0.8 and 1 in the three cases, all of them showing a rather smooth and similar behavior along the MEP. However, $i=5$ is a striking point because the three cases show a nearly zero transmission. It corresponds to the initial stage of the H_2 dissociation where a slightly elongated H_2 starts to attach to the gold wire.

To analyze this result, and based on the similarity of the three model systems considered here, we use the simplest linear model. We have calculated its eigenchannels, defined as the non-mixing transmission channels that diagonalize the transmission matrix with eigenvalues $0 \leq T_n \leq 1$, whose sum provides the total transmission of the system.³⁵⁻³⁷ For all the geometries, there is only one conduction eigenchannel contributing to the transmission at the Fermi energy, as expected for gold atomic chains. The square of the modulus of these eigenchannels provide a visualization of the electron flux through the wire, and it is plotted in 3.

Clearly, when H_2 is far from the wire ($i=1$) the conduction channel is located in the wire, 3 bottom left. When H_2 sticks to the wire, part of the electron flux passes through it, either as molecular hydrogen ($i = 8$) or as atomic hydrogen chemisorbed on the wire ($i = 27$). At $i=5$, however, the amplitude density of the eigenchannel becomes zero at the right edge, indicating that the electron flux is stopped. This reveals an interference effect.

This interference behavior can be rationalized in terms of a 4-state tight-binding model composed by 2 gold and 2 hydrogen atoms described by one orbital, where the possible electronic paths along the wire and the molecule are jointly solved. The model is defined by the energies $E_{Au}=0$ and E_H , and by three hopping terms T , $t_a = t_b$ and t (see 4). The coupling to the rest of the system is characterized by the self-energies $\Sigma_a = \Sigma_b$ associated with the a or b leads; then the wire's transmission, $T(E)$, is given by³⁸

$$T(E) = \frac{8e^2}{h} |\Sigma_a(E)|^2 |G_{ab}(E)|^2, \quad (1)$$

where $G_{ab}(E)$ is the ab -component of the Green-function associated with the four-atom model described above. 4 shows $T(E)$ for the indicated set of parameters, taking $\Sigma_a = \Sigma_b = iT$ to

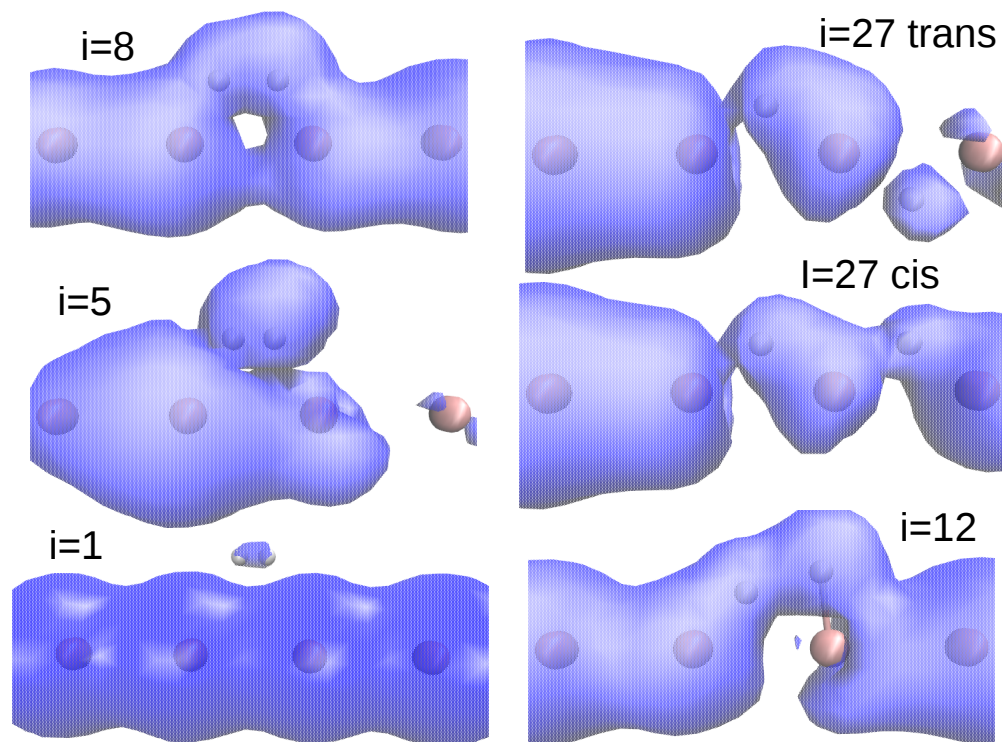


Figure 3: (Color online) Eigenchannels obtained at different i points along the MEP, for the case of the linear wire. For the MEP stage $i=5$, the electronic eigenchannel is interrupted just passed the molecule, indicating a drop in electron flux.

guarantee that $T(E = 0)$ becomes 1, for $t_a = t_b = 0$, the case of an ideal Au-chain, as in the point $i=1$. As H_2 approaches the wire, t_a grows and the electron can also be transmitted through the Au-H bond with two concurrent electron paths competing, one going through the H-atoms and the other one through the Au-atoms. There is a critical situation, when $t_a^2 = Tt$, in which the two conducting paths interfere destructively bringing the transmission to zero (see 4).³⁹⁻⁴¹ This interference is the analogue to the one manifested as a Fano profile in photoionization,⁴² when the absorption cross section presents a minimum at energies in which the direct photon excitation to a dissociative continuum (electron conduction through the gold atoms) interferes with the indirect mechanism, in which a quasi-bound state is first reached by the photon (electron localization on H atoms), and then predissociates towards the same dissociative continuum.

These conditions for the interference are imposed by the atomic geometry found in the MEP. The connection between geometry and quantum interference in molecular conduction has already

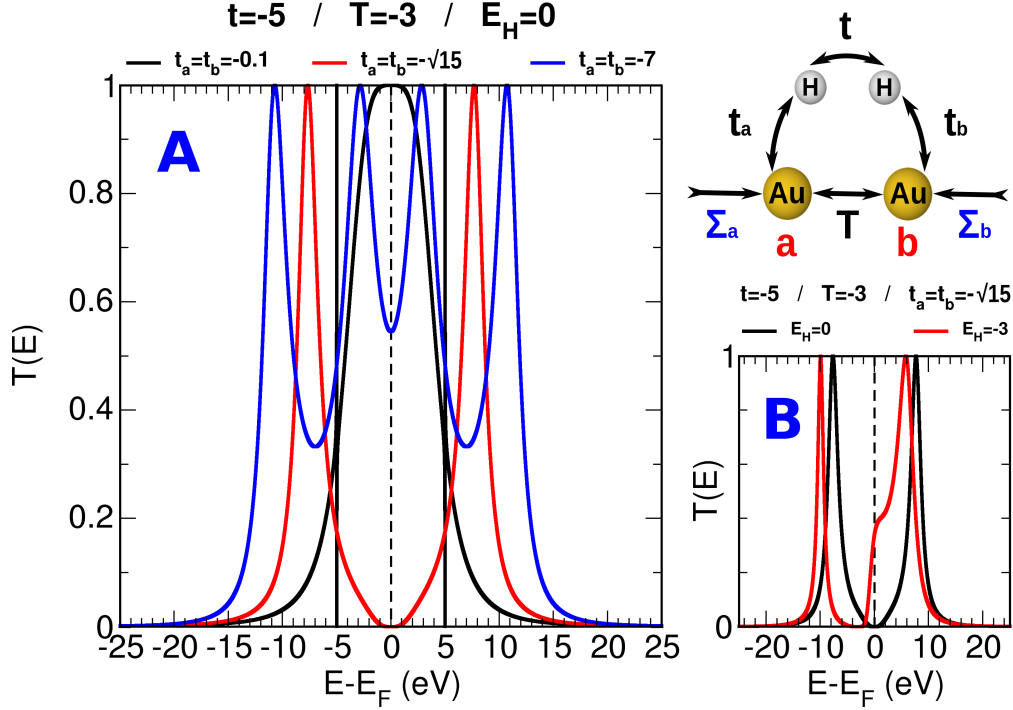


Figure 4: (Color online) Transmission as a function of energy for the model system shown in the upper right-hand side of the figure, for different values of $t_a = t_b$ and E_H ($E_{Au}=0$ eV, $T=-3$ eV and $t=-5$ eV). Panel A: $E_H=0$. Panel B: $E_H=-3$ eV. For $t_a = t_b = \sqrt{15}$, $t_a^2 = Tt$ a dip in $T(E)$ is found.

been proven experimentally.⁴³ In the present case, the H_2 -wire interactions are strong enough to steer the molecule to become parallel to the wire before dissociation. In this geometry (point $i = 5$ of the MEP), the electronic conditions needed for the above interference are met.

When studying the frozen and the relaxed nano-wires, periodic conditions on (x, y) are considered in order to build the electrodes, this permits us to define parallel k -vectors. For each (k_x, k_y) there is a similar pattern to the one discussed above for the linear case, but the position of the resonance varies with (k_x, k_y) . Thus, when averaging to get the total transmission, the zero at $i=5$ is washed out but the transmission dumps to 0.05 at the Fermi level, considerably lower than for the rest of the MEP points, 2. This indicates that the sudden decrease of the transmission persists in realistic gold wires when a molecule like H_2 approaches it.

Finite bias changes the above picture only quantitatively. The electronic transmission has been investigated at 0.5 V, 1 V and 2 V. This has been done at the configurations of the MEP calculated for zero voltage. At finite bias, the MEP is ill-defined due to the appearance of non-conservative

forces.^{44–46} However, if the bias-induced changes in the forces are small enough, we expect the zero-voltage MEP to be an excellent approximation to the molecular path at low temperatures. Indeed, this is the case. In order to show this, we studied the minima, points $i=8$ and 27 of Γ . These points correspond to equilibrium geometries and are then very sensitive to variations of the forces. The bias-induced forces were negligible and the equilibrium geometries analyzed were the same as for zero bias.

For 2 V , the wire is reaching its stability limit and it is expected to break.⁴⁷ In this case, the system undergoes important changes diverging from the zero-voltage MEP. For $i=8$ the two hydrogen atoms trend to insert themselves in the gold wire, producing a separation of the two closest gold atoms. For $i=27$, one hydrogen atom moves to the other side of the wire, towards a *trans* configuration. Hence, the electron-transmissions evaluated for the zero-voltage MEP, while correct at 1 V , are just of academic interest at 2 V .

Γ shows the wire's currents evaluated from the electron transmissions for 1 and 2 V . As voltage increases, the current increases as well. For all the considered wire models, there is a pronounced decrease of the current intensity for $i=5$. Again, we retrieve that the decrease is due to the quantum-interference effect at the initial stage of dissociation. These results show that even at biases larger than 1 V , within the stability limit of the wire, the dissociation of the H_2 molecule will cause a measurable decrease in the electron current through the gold wire.

In summary, non-equilibrium Green's functions (NEGF) calculations based on density functional theory (DFT) are used to evaluate the minimal energy path (MEP) that an H_2 molecule follows near an atomic-sized gold wire. The molecule dissociates on the wire and the electronic current decrease in the initial stages of H_2 dissociation on a gold atomic wire. This current drop is due to quantum interference between electron paths when the molecule starts interacting with the gold wire. Moreover, no significant dependence of the MEP on applied biases below the wire's stability limit has been found. This suggests that the conductance properties of gold wires can be recorded to acquire information on chemical reactions taken place in the single-molecule limit in a gas or liquid environment.

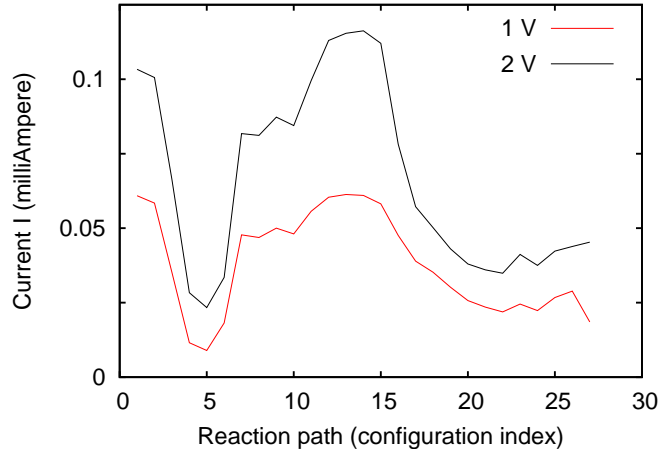


Figure 5: (Color online) Electron current, I , for biases of 1 V and 2 V, versus the system configurations, which correspond to the zero-bias MEP for the relaxed wire, 1. At the dissociation onset, stage $i=5$, there is an important drop in the current due to quantum interference between the through-wire and through-molecule electron paths. The drop is visible at both biases. At 2 V, the wire's stability is compromised and the zero-bias MEP is used for illustration of the robustness of the quantum interference effect.

This work has been supported by Comunidad Autónoma de Madrid (CAM) under Grant No. S-2009/MAT/1467, by the Ministerio de Ciencia e Innovación under Grant No. FIS2011-29596-C02, and by the European-Union Integrated Project AtMol (<http://www.atmol.eu>). We would like to thank as well the CESGA computing centre for the computing time under the ICTS grants.

References

- (1) Eigler, D.; Lutz, C.; Rudge, W. *Nature* **1991**, 352, 600–603.
- (2) Dujardin, G.; Walkup, R.; Avouris, P. *Science* **1992**, 255, 1232–1235.
- (3) Gimzewski, J.; Joachim, C.; Schlittler, R.; Langlais, V.; Tang, H.; Johannsen, I. *Science* **1998**, 281, 531–533.
- (4) Hla, S.-W.; Bartels, L.; Meyer, G.; Rieder, K.-H. *Phys. Rev. Lett.* **2000**, 85, 2777–2780.
- (5) Lee, H.; Ho, W. *Science* **1999**, 286, 1719–1722.

- (6) Sainoo, Y.; Kim, Y.; Okawa, T.; Komeda, T.; Shigekawa, H.; Kawai, M. *Phys. Rev. Lett.* **2005**, *95*, 246102.
- (7) Kumagai, T.; Shiotari, A.; Okuyama, H.; Hatta, S.; Aruga, T.; Hamada, I.; Frederiksen, T.; Ueba, H. *Nature Materials* **2012**, *11*, 167–172.
- (8) Schaffert, J.; Cottin, M. C.; Sonntag, A.; Karacuban, H.; Bobisch, C. A.; Lorente, N.; Gauguier, J.-P.; Moeller, R. *Nature Materials* **2013**, *12*, 223–227.
- (9) Hla, S. W.; Braun, K. F.; Wassermann, B.; Rieder, K. H. *Physical Review letters* **2004**, *93*, 208302.
- (10) Komeda, T.; Kim, Y.; Kawai, M.; Persson, B.; Ueba, H. *Science* **2002**, *295*, 2055–2058.
- (11) Pascual, J. I.; Lorente, N.; Song, Z.; Conrad, H.; Rust, H. P. *Nature* **2003**, *423*, 525–528.
- (12) Hutchings, G. J. *J. Catal.* **1985**, *96*, 292.
- (13) Haruta, M.; Yamada, N.; Kobayashi, T.; Iijima, S. *J. Catal.* **1989**, *115*, 301.
- (14) Sanchez, A.; Abbet, S.; Heiz, U.; W.-D. Schneider, H. H.; N, R.; Barnett,; Landman, U. *J. Phys. Chem. A* **1999**, *103*, 9573.
- (15) Häkkinen, H.; Landman, U. *Phys. Rev. B* **2000**, *62*, R2287.
- (16) Häkkinen, H.; Moseler, M.; Landman, U. *Phys. Rev. Lett.* **2002**, *89*, 033401.
- (17) Gilb, S.; Weis, P.; Furche, F.; Ahlrichs, R.; Kappes, M. M. *J. Chem. Phys.* **2002**, *116*, 4094.
- (18) Furche, F.; Ahlrichs, R.; Weis, P.; jacob, C.; Gilb, S.; Bierweiler, T.; Kappes, M. M. *J. Chem. Phys.* **2002**, *117*, 6982.
- (19) Fernández, E. M.; Soler, J. M.; Garzón, I. L.; Balbás, L. C. *Phys. Rev. B* **2004**, *70*, 165403.
- (20) Gruene, P.; Rayner, D. M.; Redlich, B.; van der Meer, A. F. G.; Lyon, J. T.; Maijer, G.; Fielicke, A. *Science* **2008**, *321*, 674.

- (21) Lechtken, A.; Neiss, C.; Kappes, M. M.; Schooss, D. *Phys. Chem. Chem. Phys.* **2009**, *11*, 4344.
- (22) Yanson, A. I.; Bollinger, G. R.; van den Brom, H. E.; Agrait, N.; van Ruitenbeek, J. M. *Nature* **1998**, *395*, 783.
- (23) Ohnishi, H.; Kondo, Y.; Takayanagi, K. *Nature* **1998**, *395*, 780.
- (24) Häkkinen, H.; Barnett, R. N.; Landman, U. *J. Phys. Chem. B* **1999**, *103*, 8814.
- (25) Bahn, S. R.; Lopez, N.; Norskov, J. K.; Jacobsen, K. W. *Phys. Rev. B* **2002**, *66*, 081405(R).
- (26) Legoas, S. B.; Galvao, D. S.; Rodrigues, V.; Ugarte, D. *Phys. Rev. Lett.* **2002**, *88*, 076105.
- (27) Csonka, S.; Halbritter, A.; Mihály, G.; E. Jurdik, O. S.; Speller, S.; van Kempen, H. *Phys. Rev. Lett.* **2003**, *90*, 116803.
- (28) Barnett, R. N.; Häkkinen, H.; Scherbakov, A. G.; Landman, U. *Nano Lett.* **2004**, *4*, 1845.
- (29) Frederiksen, T.; Paulsson, M.; Brandbyge, M. *J. Phys.* **2007**, *61*, 312.
- (30) Jelínek, P.; Pérez, R.; Ortega, J.; Flores, F. *Phys. Rev. Lett.* **2006**, *96*, 046803.
- (31) Zanchet, A.; Dorta-Urra, A.; Roncero, O.; Flores, F.; Tablero, C.; Panigua, M.; Aguado, A. *Phys. Chem. Chem. Phys.* **2009**, *11*, 10122.
- (32) Soler, J. M.; Artacho, E.; Gale, J.; García, A.; Junquera, J.; Ordejón, P.; Sánchez-Portal, D. *J. Phys.: Condens. Matter* **2002**, *14*, 2745.
- (33) Brandbyge, M.; Mozos, J. L.; Ordejón, P.; Taylor, J.; Stokbro, K. *Phys. Rev. B* **2002**, *65*, 165401.
- (34) Perdew, J. P.; Burke, K.; Ernzerhof, M. *Phys. Rev. Lett.* **1996**, *77*, 3865.
- (35) Mujica, V.; Kemp, M.; Ratner, M. A. *J. Chem. Phys.* **1994**, *101*, 6849.

- (36) Kopf, A.; Saalfrank, P. *Chem. Phys. Lett.* **2004**, 386, 17.
- (37) Paulsson, M.; Brandbyge, M. *Phys. Rev. B* **2007**, 76, 115117.
- (38) Fisher, D. S.; Lee, P. A. *Phys. Rev. B* **1981**, 23, 6851.
- (39) Solomon, G. C.; Herrmann, C.; Hansen, T.; Mujica, V.; Ratner, M. A. *Nature Chemistry* **2010**, 2, 223–228.
- (40) Guédon, C. M.; Valkenier, H.; Markussen, T.; Thygesen, K. S.; Hummelen, J. C.; van der Molen, S. J. *Nature Nanotechnology* **2012**, 7, 305–309.
- (41) Markussen, T.; Stadler, R.; Thygesen, K. S. *Phys. Chem. Chem. Phys.* **2011**, 13, 14311.
- (42) Fano, U. *Phys. Rev.* **1961**, 124, 1866.
- (43) Aradhya, S. V.; Meisner, J. S.; Krikorian, M.; Ahn, S.; Parameswaran, R.; Steigerwald, M. L.; Nuckolls, C.; Venkataraman, L. *Nano Letters* **2012**, 12, 1643–1647.
- (44) Dundas, D.; McEniry, E. J.; Todorov, T. N. *Nature Nanotechnology* **2009**, 4, 99–102.
- (45) Todorov, T. N.; Dundas, D.; McEniry, E. J. *Phys. Rev. B* **2010**, 81, 075416.
- (46) Lü, J.-T.; Brandbyge, M.; Hedegaard, P. *Nano Letters* **2010**, 10, 1657–1663.
- (47) Yasuda, H.; Sakai, A. *Phys. Rev. B* **1997**, 56, 1069.